Enhanced Membrane Permeabilization and Antibacterial Activity of a Disulfide-Dimerized Magainin Analogue

Christopher E. Dempsey,* Shohta Ueno, and Matthew B. Avison

Biochemistry Department and Molecular Recognition Centre, Bristol University, School of Medical Sciences, University Walk, Bristol BS8 1TD, U.K.

Received June 19, 2002; Revised Manuscript Received November 1, 2002

ABSTRACT: A cysteine substitution analogue of magainin-2 amide (magainin-F12W, N22C; denoted here as mag-N22C), and a disulfide-linked dimer prepared by air oxidation [(mag-N22C)$_2$], were compared in their ability to release carboxyfluorescein (CF) from 100-nm large unilamellar vesicles (LUV) and to kill the Gram negative bacteria *Stenotrophomonas maltophilia* and *Escherichia coli*. The disulfide-dimerized peptide showed enhanced permeabilization and antimicrobial activity, when compared with the monomeric peptide, that was particularly marked at very low peptide concentrations. The enhanced CF-releasing activity of the dimer at low concentrations in vesicles results from (i) enhanced binding to negatively charged membrane surfaces and (ii) a low concentration dependence for permeabilization in the dimer compared to the monomer. The unique properties of the dimeric peptide suggest a role for structural diversity of antimicrobial peptides in frog skin, including the recent identification of a heterodimer composed of disulfide-linked amphipathic helical peptides [Batista et al. (2001) *FEBS Lett. 494*, 85−89]. Disulfide-dimerization of pore-forming, positively charged, amphipathic helical peptides may be a useful general approach to the generation of peptide antimicrobials having activity at very low concentrations.

Animals contain a diverse array of antimicrobial peptides that contribute to their innate immunity or to a first line of defense against opportunistic bacterial infections (*1*). Antimicrobial peptides have been well characterized in frog skin, which secretes a wide diversity of different peptides (*2*). This diversity may result from as yet uncharacterized specificity against different pathogens. It has also been shown that some of the diversity found in several classes of antimicrobial peptides that form amphipathic helical conformations on binding to membranes may be due to specific synergistic effects (*3*). Thus, the frog skin magainin/PGLA pair of membrane-binding helical peptides have greater than additive effects when tested for membrane pore formation in vesicles composed of negatively charged lipids (*4*−*6*). This synergism has been proposed to result from pairwise interaction of the peptides in membranes (*6*), and recent studies have indicated that magainin and PGLA do form a parallel (rather than antiparallel) 1:1 association in negatively charged membranes (*7*). Since each peptide is known to bind to membranes *at equilibrium* in the interfacial region parallel to the membrane surface (*8*, *9*), it is assumed that the parallel association of helices also occurs at the membrane surface. This pairwise interaction in some way promotes or stabilizes the membrane pore. A general membrane perturbation that should result from the pairwise association of amphipathic helical peptides at the membrane interface has been described based on membrane perturbation and pore formation of disulfide-dimerized melittin analogues (*10*, *11*).

In light of these observations, the recent identification of a frog skin peptide comprising two putative membrane binding amphipathic helical peptides linked by a disulfide bond is intriguing (*12*). To characterize the properties of disufide-paired antimicrobial peptides of this type, we have prepared a C-terminally disulfide-dimerized analogue of magainin and determined its membrane binding and permeabilizing properties in vesicles, and its antimicrobial activity against the Gram negative bacteria *Stenotophomonas maltophilia* and *Escherichia coli*. *S. maltophilia* is an important emerging human pathogen that infects a large number of immunocompromised hospital patients each year. Particularly worrying is the multidrug resistance nature of *S. maltophilia*, some isolates being resistant to all clinically available antibiotics (*13*). The unique properties of the dimeric peptide in both its permeabilizing and antimicrobial activity against this pathogen, and other Gram-negative bacteria, give some insight into the possible role of the diversity of frog skin peptides in broadening the scope of the innate immune response.

EXPERIMENTAL PROCEDURES

Peptide Synthesis. The cysteine-replacement analogue of magainin2 amide (magainin-F12W, N22C amide; see sequence in Figure 1), designated here as mag-N22C,[1] was prepared by solid-phase synthesis using Fmoc chemistry by Dr. Graham Bloomberg of the Bristol Centre for Molecular

* To whom correspondence should be addressed. E-mail: c.dempsey@bris.ac.uk. Tel: (0)117 928 7427. Fax: (0)117 28 8274.

[1] Abbreviations: CD, circular dichroism; CF, carboxyfluorescein; EDTA, ethylenediaminetetraacetic acid; FPE, fluorescein-phosphatidylethanolamine; HPLC, high performance liquid chromatography; LUV, large unilamellar vesicle; mag-N22C, GIGKFLHSAKKWGKAFVGEIMCS-amide; (mag-N22C)$_2$, disulfide dimerised version of mag-N22C; PBS, phosphate buffered saline; TBS, tris buffered saline; PC, phosphatidylcholine; PG, phosphatidylglycerol; TFA, trifluoroacetic acid.

10.1021/bi026328h CCC: $25.00
Published on Web 12/14/2002

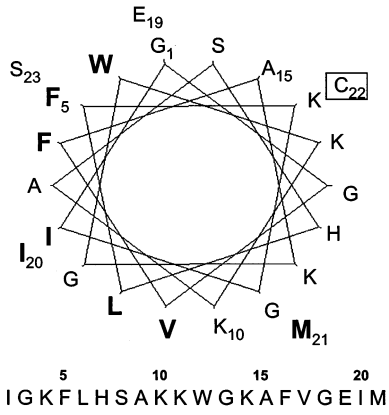

FIGURE 1: Amino sequence of mag-N22C. In the helical wheel representation, the amino acids with bulky hydrophobic side chains are noted in heavy type and the Cys-22 residue (replacing Asn in the natural sequence) is highlighted. $(mag\text{-}N22C)_2$ is a dimeric version of the sequence shown, prepared by disulfide formation at residue C22.

Recognition. The peptide was purified by HPLC using a water (0.1% trifluoroacetic acid)−acetonitrile (0.1% TFA) gradient (20−40% acetonitrile during 20 min). The dimeric peptide [$(mag\text{-}N22C)_2$] was prepared by incubating the purified monomer at a concentration of 1 mg mL^{-1} in aerated 10 mM Tris-HCl buffer pH 9.0 containing 0.5 mM EDTA for 24 h at room temperature. The dimerized peptide was purified by HPLC using the same gradient as above. The monomeric (mag-N22C) and disulfide-dimerized peptide [$(mag\text{-}N22C)_2$] were greater than 95% pure as judged by analytical HPLC, and had the correct atomic mass as determined by matrix assisted laser desorption ionization mass spectrometry [mag-N22C, theoretical mass = 2494 D, experimental mass 2493.8 D; $(mag\text{-}N22C)_2$, theoretical mass 4986 D, experimental mass 4987.1 D]. In all experiments described, samples of mag-N22C (monomer) contained a 2-fold molar excess of dithiothreitol that was included in stored stock solutions to prevent disulfide dimerization. Control experiments showed that neither vesicle dye release, membrane binding, antimicrobial activity, nor hemolysis activity was affected by dithiothreitol at the highest concentrations utilized in the experiments. After each series of experiments, the peptide stock solutions were checked by HPLC to confirm the integrity of the peptides.

Preparation of Lipid Vesicles. Large unilamellar vesicles (LUV) of 100 nm diameter were prepared from equimolar egg PC and egg PG (Lipid Products, Nutfield, U.K.). Solutions of the lipids in chloroform/methanol, 1:1, were mixed to the desired composition, dried under a stream of nitrogen, and the residual solvent was removed by pumping under high vacuum for at least 4 h. The lipids were hydrated in sample buffer (10 mM Tris-HCl, pH 7.4; 1 mM EDTA) at a total lipid concentration of 10 mg mL^{-1}, freeze−thawed three times, and pressure-extruded 10 times through two 100-nm pore membranes, using a Lipex Biomembrane extruder (Vancouver, Canada). LUV loaded with carboxyfluorescein (CF; Sigma Chemical Co.) were prepared by hydrating the dried lipids in sample buffer containing 50 mM CF. After extrusion, the vesicles were separated from external CF by gel filtration in sample buffer containing 107 mM NaCl to balance osmotically the internal CF. All experiments with vesicles were made in sample buffer containing 107 mM NaCl (high salt buffer). The fluorescence binding experiments and circular dichroism experiments described below employed vesicles in which internal CF was replaced with 107 mM NaCl, so that in all experiments, the internal and external media were osmotically equivalent. LUV containing membrane-incorporated fluorescein-phosphatidylethanolamine (FPE) (*14*) were prepared by adding 10 μL of a 10 mg mL^{-1} FPE solution in ethanol, to 400 μL of LUVs (10 mg mL^{-1} total lipid) prepared in high salt buffer, shaking and incubating at 35 °C for 40 min, followed by gel filtration to remove ethanol and unincorporated FPE. Absorption spectroscopy of the resulting vesicles indicated that FPE incorporation into the bilayers was between 1:300 and 1:600 (FPE/lipid; mol/mol). Small unilamellar vesicles (SUV) for circular dichroism experiments were prepared as described for LUV except that freeze thawed lipid samples were sonicated using a Branson tip sonicator in 30 s bursts on ice until the samples were optically clear, followed by centrifugation to remove debris.

Fluorescence Spectroscopy. Fluorescence spectra were measured using a Perkin-Elmer LS50B fluorimeter. All peptide solutions were made in plastic sample tubes or cuvettes to avoid loss of peptide at low concentrations due to binding to glass surfaces. For the measurement of vesicle-induced changes in the emission spectrum of the Trp-12 residue, a 2 μM peptide sample (peptide concentrations are based on magainin monomers; i.e., the dimer concentration was 1 μM in dimer and 2 μM in terms of monomer subunits) was incubated in high salt sample buffer, and aliquots of a vesicle suspension were added to give total lipid concentrations in the range 0 to 50 μM. The concentration of lipids in the stock solution was adjusted so that changes in total volume of the sample were less than 0.5%. Tryptophan fluorescence was excited at 280 nm, and the emission spectrum was measured between 300 and 450 nm in 1 nm intervals with 1 s signal averaging. Emission spectra obtained from 2 μM tryptophan (which does not bind to vesicles under these conditions) in the presence of vesicles at 100 μM total lipid concentration, showed that light scattering artifacts were negligible. Peptide membrane binding affinities are expressed as mole fraction partition coefficients obtained by fitting fluorescence data to eq 1,

$$\Delta\lambda = \frac{\Delta\lambda_{max} K_x [L]}{([W] + K_x [L])} \quad (1)$$

where $\Delta\lambda$ is the change in fluorescence emission wavelength upon peptide binding, $\Delta\lambda_{max}$ is the maximum change in the emission wavelength, [L] is the total lipid concentration, [W] is the concentration of water (55.3 M), and K_x is the mole fraction partition coefficient that defines the partitioning of peptide between the aqueous and lipid phases (*15*).

Peptide-induced dye release from vesicles loaded with CF was measured from the loss of fluorescence self-quenching as the dye was diluted into the extravesicular solution. Emission was measured at 520 nm (excitation at 490 nm), and the slit widths were adjusted so that the maximum fluorescence upon total release of CF (obtained by adding 10 μL of 20% Triton X100) was less than 1000. To ensure rapid mixing of peptide and vesicles, and to avoid local high peptide concentrations, 1 mL of a peptide solution at double the post-mix concentration was rapidly ejected from an

Eppendorf pipet into 1 mL of a vesicle suspension at 130 μM total lipid concentration (65 μM post mix) to initiate binding and dye release.

Peptide binding to FPE-labeled vesicles was measured by adding aliquots of peptide to a suspension of vesicles in high salt sample buffer (total lipid concentration was 65 μM). FPE emission was measured at 520 nm (excitation at 490 nm). The experiments for which data are shown in the figures were made by adding successive aliquots of peptide to a single vesicle sample. Control experiments showed that the same fluorescence changes were produced on adding either a large aliquot of peptide or the same total peptide concentration in successive small aliquots, consistent with rapid equilibration of peptide throughout the vesicle population.

Residual Quenching in Vesicle Populations Partially Depleted of Internal CF. Residual CF self-quenching factors in partially CF-depeleted vesicles were determined using the method of Schwarz and colleagues (*16*, *17*). Peptide concentrations, and CF release times were chosen, based on the dye release experiments described in the previous section, to give vesicle populations having approximately 50, 40, 30, 20, and 10% total residual vesicle-trapped CF. Dye release in these experiments was monitored fluorimetrically, and CF release was quenched at appropriate times by the addition of a concentrated suspension of dye-free vesicles in high salt sample buffer equivalent to a 10-fold excess of total lipid. Aliquots (0.75 mL) of the vesicles were isolated from released CF by gel filtration, the volume was made to 1.5 mL with high salt buffer, and the residual quenching was measured from the fluorescence intensity before and after addition of an aliquot of Triton X-100 as described in the previous section.

Circular Dichroism Spectroscopy. Circular dichroism spectra were obtained at 20 °C using a Jobin-Yvon CD6 spectropolarimeter. Spectra were obtained in sample buffer containing 150 mM NaCl. Spectra of isolated peptides were obtained in 2-mm path length quartz cuvettes; spectra of samples containing peptide and SUV were obtained in 0.1-mm path length quartz cuvettes. All spectra are averages of between three and five scans with relevant (peptide-free) blank spectra subtracted, and were zeroed at 260 nm before plotting without smoothing.

Antibacterial Assay. The test bacterium, *Stenotrophomonas maltophilia* or *E. coli* (strains DH5α or JM105), was grown in standard rich growth media (nutrient broth, Oxoid plc. UK) overnight, with seeding from a single colony in the absence of antibiotics. Growth was at 37 °C with vigorous shaking. From the overnight, turbid culture, 100 μL was taken to innoculate fresh 10 mL nutrient broth cultures. Peptide was then added to a final concentration range of 0−5.0 μM monomer equivalents, and incubations were continued for 1 h at 37 °C with shaking. Following incubation, a viable count was determined by diluting the culture appropriately with nutrient broth and plating out an appropriate amount of culture onto a nutrient agar plate. The aim was to give less than 1000 colonies per plate. Plates were incubated for 48 h at 30 °C in air and the number of colonies harbored by each was counted. Taking into consideration the recorded dilution factor, the viable count (i.e., the number of live bacteria/mL in the culture following incubation with or without peptide) was determined. Data presented are the averages of three separate experiments.

Hemolysis Assay. Recently outdated human red blood cells were washed three times in phosphate buffered saline (PBS; 35 mM phosphate, 150 mM NaCl, pH 7.3), followed by one wash in Tris-buffered saline (TBS; 35 mM Tris-HCl, 150 mM NaCl, pH 7.3). The red blood cells were finally resuspended in TBS at 2% hemocrit. Hemolysis was determined by mixing 100 μL of RBC with 100 μL of a solution of peptide in TBS to give the final peptide concentration required. The samples were incubated at 37 °C for 30 min, and the extent of hemolysis was determined by diluting 100 μL into 900 μL of TBS, pelleting the cells, and measuring the absorbance at 578 nm due to released hemoglobin. Activity of each peptide at each concentration is expressed as the percentage of total hemoglobin released (100% release was measured by incubating RBC with 20 μM melittin). TBS (rather than PBS) was used in all experiments where comparisons with melittin were made, since melittin-induced hemolysis is suppressed by phosphate, which promotes the self-associated (inactive) form of the peptide. Control experiments showed that hemolysis induced by either mag-N22C or $(\text{mag-N22C})_2$ was the same in TBS compared with PBS. Each measurement was made in duplicate.

RESULTS

Peptide-Design and Structure. Magainin peptides in a helical conformation are highly amphipathic (Figure 1). In negatively charged membranes, at equilibrium, the peptides bind in the interfacial region of the bilayer with the helix axis parallel to the peptide plane and the hydrophobic surfaces oriented toward the membrane interior (*8*, *9*). In aqueous solution at low concentrations, they are unstructured. Previous studies with disulfide-dimerized melittins (*10*, *11*, *18*) indicated this characteristic membrane-induced transition from an unstructured to an amphipathic helical conformation, is retained when a disulfide bond is placed near the peptide C-terminus and away from the potential hydrophobic helical surface. A disulfide bond linking the hydrophobic faces of potential amphipathic helices can induce structure in the peptide dimer in solution (*18*). We therefore replaced Asn-22 [on the polar helix face (Figure 1)] with Cys, to form the disulfide-linked dimer. As described in the discussion, it is likely that the C-terminal 3−4 residues of the monomeric and disulfide-linked dimer do not adopt a helical conformation when the peptides are bound at the membrane interface.

Circular dichroism spectra (Figure 2a) of mag-N22C and $(\text{mag-N22C})_2$ in sample buffer containing 150 mM NaCl (the buffer used in the dye-release experiments of Figures 3−5) indicate that each peptide has negligible helix content at concentrations (20 μM) well above those used in the dye release experiments. In membranes having the same composition as used in the dye release measurements (Figures 3−5), the peptide monomer and dimer have virtually indistinguishable circular dichroism spectra (Figure 2b), indicating that the helical content of the membrane-bound monomer is unaffected by cross linking in a disulfide-linked dimer. As with other magainins, the peptide monomer and dimer are around 65−70% helical in the membrane bound state. These results indicate that the disulfide bond is accommodated with the retention of the essential features (membrane-induced induction of helix

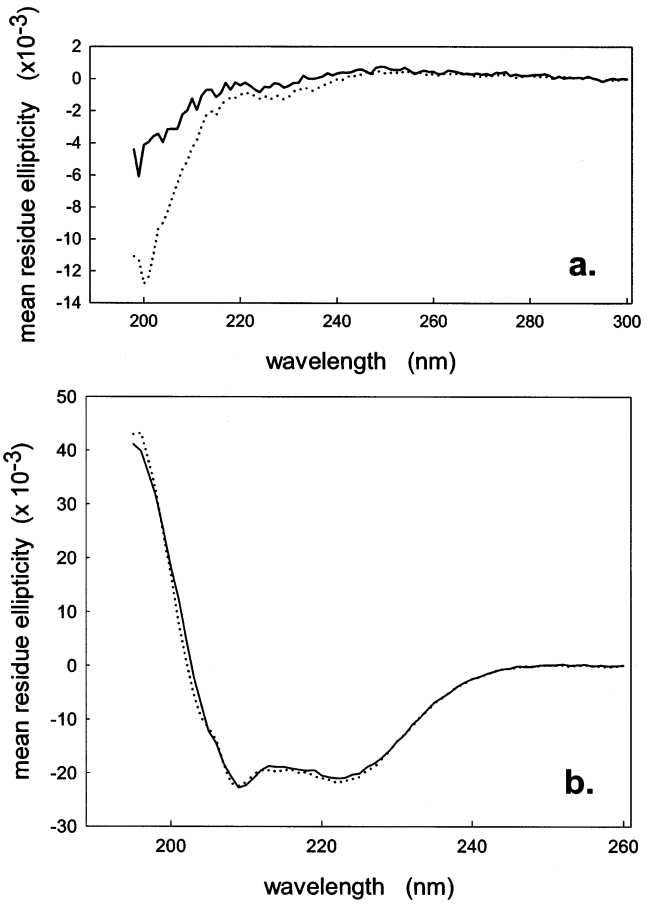

FIGURE 2: (a) Circular dichroism spectra of mag-N22C (solid line) and $(mag\text{-}N22C)_2$ (dotted line) in 10 mM Tris HCl, pH 7.4 containing 150 mM NaCl and 1 mM EDTA, at 20 °C. In each case, the peptide concentration was 16 μM (based on monomer units; i.e. the absolute dimer concentration was 8 μM). (b) Circular dichroism spectra of mag-N22C (solid line) and $(mag\text{-}N22C)_2$ (dotted line) in buffer at a concentration of 100 μM (in monomer units) containing SUV composed of egg PC/egg PG; 1:1, mol/mol) at a total lipid concentration of 10 mM.

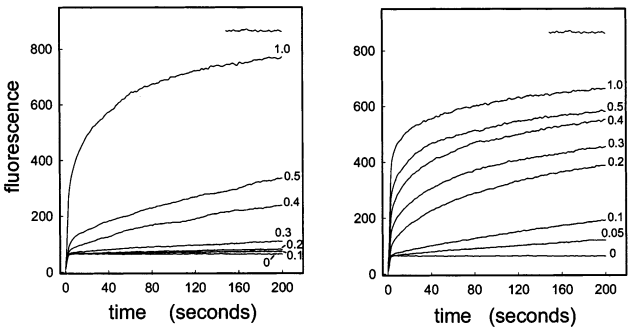

FIGURE 3: Time dependence of the fluorescence increase resulting from peptide-induced pore-formation in 100 nm large unilamellar vesicles composed of equimolar PC and PG in high salt sample buffer (see text). The left-hand panel is data for mag-N22C monomer; the right-hand panel is dye release induced by $(mag\text{-}N22C)_2$ (disulfide-linked dimer). The total lipid concentration was 65 μM in each experiment and each dye release curve is annotated with the peptide concentration in micromolar *monomer* units (i.e., the absolute dimer molar concentrations are 0.5 times those indicated in the right panel). The top truncated line is the fluorescence level resulting from complete dye release upon adding an aliquot of detergent sufficient to solubilize the lipid.

corresponding to around 65−70% of the residues of the peptide) of the peptide monomer.

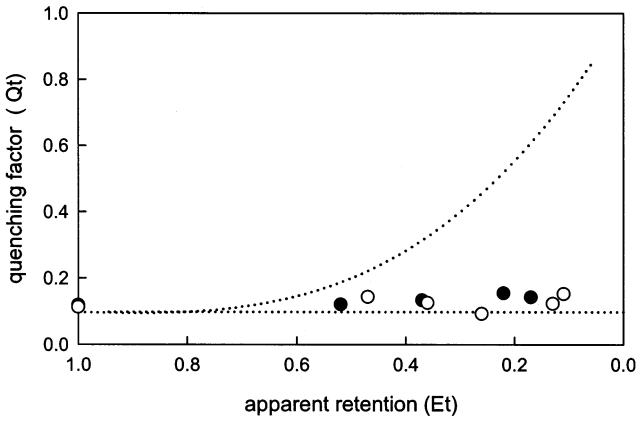

FIGURE 4: Residual quenching factors (Qt) in CF-containing vesicles after treatment with peptide [mag-N22C (filled circles) and $mag(N22C)_2$ (open circles)] at concentrations sufficient to release total CF in the vesicle population to the level indicated by Et. A value of Et of 0.2 indicates, for example, that 80% of the total intravesicular CF in the vesicle population has been released. The lower (horizontal) dotted line indicates the residual quenching factor (Qt) expected if the residual intravesicular CF is maximally quenched ("all or nothing" release). The upper dotted curve indicates the values of Qt expected for "graded release", i.e., the proportion of residual intravesicular dye in *individual* vesicles is the same as the value determined for the entire vesicle population. The latter curve was obtained by fitting measured quenching factors in vesicles containing known concentrations of CF to a polynomial function as described in ref *17*.

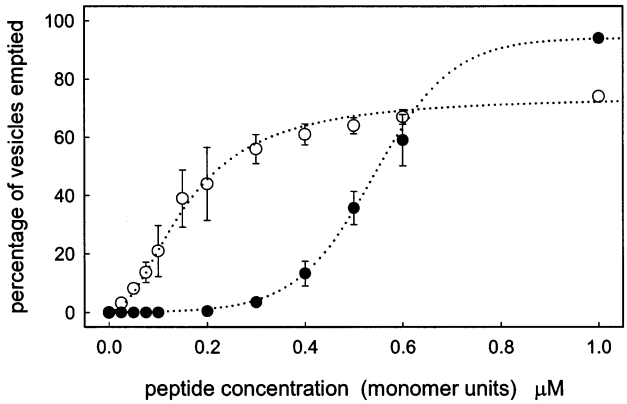

FIGURE 5: Percentage of vesicles emptied of internal carboxyfluorescein as a function of peptide concentration (in monomer units), measured 200 s after mixing. Data for mag-N22C (filled circles) and $(mag\text{-}N22C)_2$ (open circles) are averages (with standard deviations) of two or three measurements from three separate experiments. Dotted lines are fits to sigmoidal functions of the form $P = P_{max}ac^n/(b + ac^n)$, where P is the percentage of vesicles emptied, P_{max} is the maximum value of P, c is the peptide concentration, and a and b are constants. The values of n are 5.3 and 2.0 for the monomer and dimer, respectively.

Dye Release from LUV Composed of Mixed Neutral and Negatively Charged Lipids. Figure 3 illustrates the fluorescence increase in suspensions of CF-loaded vesicles that results from peptide-induced leakage of dye into the extravesicular solution where self-quenching is abolished. Detectable dye release is observed for mag-N22C only at concentrations of around 0.2 μM and higher, whereas dye release from vesicles resulting from effects of the disulfide-linked dimer $[mag\text{-}N22C)_2]$ is observed at concentration of 0.025 μM (based on monomer units; i.e., the *molar* dimer concentration is 0.0125 μM). This corresponds to around 1 *dimer* per 5000 membrane lipid molecules. Peptide-induced dye

release displays two phases under these conditions, a very rapid initial release followed by a slow rate of release that tends to a steady state. In many studies, the release data are converted to pore formation rates using formalisms described by Schwarz (*16*), from which the concentration-dependence of pore formation can give insight into the molecularity of rate-limiting steps (*10*, *17*). In the case of magainin interactions with vesicles containing negatively charged lipid, this analysis is not justified because of the extremely rapid binding of positively charged peptide to the negatively charged membrane surface, that occurs much more quickly than manual mixing even under the most favorable conditions. Stop flow rapid mix experiments show that peptide binding to vesicles having the lipid composition described here occurs with a rate constant greater than 100 s^{-1} (unpublished results), whereas equilibration of peptide and lipid cannot be achieved by manual mixing in less than a second. We have chosen, therefore, to represent the dye release data as dose response curves correlating the proportion of total entrapped dye released as a function of peptide concentration (see Figure 5). This is more realistic in comparison with antibacterial effects of the peptides, which, of course, are not measured by rapid mixing.

Both mag-N22C and $(mag\text{-}N22C)_2$ release dye from 100 nm LUVs with close to "all or nothing" kinetics as determined by the measurement of residual quenching factors in vesicles isolated after incubation with peptide (*16*) (Figure 4). Even at very high levels (80−90%) of depletion of trapped dye *within a vesicle population*, the residual entrapped dye *in individual vesicles* is highly quenched. This indicates that the vesicle population consists of vesicles that are either intact or are largely depleted of dye. In other words, a single lytic event is sufficiently long-lived, relative to the diffusion rate of dye through the membrane opening, to deplete the vesicle in a single event. Under "all or nothing" kinetics, the proportion of total CF released from a vesicle population is equivalent to the proportion of vesicles emptied (Figure 5).

The dose−response data of Figure 5 demonstrate that membrane permeabilization and dye release induced by mag-N22C shows a sigmoidal dependence on peptide concentration, whereas that induced by the dimerized peptide has a dependence on peptide concentration that is considerably less sigmoidal. The observation of a threshold in monomer concentration below which dye release is absent, together with a steep concentration dependence between 0.4 and 0.8 μM peptide, is characteristic of a requirement for peptide self-association in assembly of a "pore". According to fits of the dose−response data to a sigmoidal function (see Figure 5 legend), the percentage of vesicles emptied varies with approximately a fifth order dependence ($n = 5.3$) on the monomer concentration and a second order dependence on dimer concentration ($n = 2.0$). We emphasize that these are only approximate indications of the molecularity of the peptide-induced permeabilization, due to the difficulty of obtaining good mixing of peptide with vesicles relative to the time scale of binding (see above). For example, we routinely find that the dimer permeabilizes well below 100% of the vesicles in a sample even at rather high peptide concentration, whereas all the vesicles are permeabilized by the monomer (see Figure 5), an observation we ascribe to the inability to completely equilibrate dimer and vesicles before binding in a manual mix. However, the data summarized in Figure 5 are generally consistent with previous estimates of a fourth to fifth order dependence of pore formation on magainin concentration in negatively charged vesicles (*19*), and with the expectation that linking vesicle bound monomers into dimers will lower the molecularity of any process (like pore formation) requiring self-association of monomers. Although the monomer and dimer share similar structural (Figure 2) and permeabilization properties (Figures 3 and 4), the extent to which the dimer generates the type of discrete pore comprising transient transmembrane oriented helical monomers in a toroidal lipid−peptide co-assembly proposed for magainin (*20*, *21*) has not been determined. We therefore use the term "permeabilization" to describe peptide-induced dye release in this study, although it is likely that at least the monomeric peptide acts by forming a "pore" of the type described by Matsuzaki and Huang (*20*, *21*).

Binding of Monomeric and Dimeric Magainin to Vesicles. An alternative explanation for sigmoidal dose response curves is cooperative binding of monomer to the membrane surface (*22*). We have tested this by measuring membrane binding in two ways, as shown in Figure 6. As the peptide binds to the membrane surface, the Trp-12 fluorescence emission undergoes a blue spectral shift characteristic of transfer to a less polar environment. This can be used to determine a binding curve by titrating solutions of the peptide with vesicles. Figure 6a shows that each peptide displays hyperbolic binding properties indicating a lack of cooperativity in membrane binding. As expected for binding of positively charged peptide to negatively charged vesicles, binding is very tight, even in 107 mM NaCl. The mole fraction partition coefficients K_x, determined by fitting to eq 1 are 5.4×10^6 (monomer) and 12.6×10^6 (dimer). These values may be compared with the mole fraction partition coefficient for binding of melittin (having a similar overall amphipathicity and positive charge as magainin) to *neutral* vesicles of around 10^5 (*23*). Disulfide-dimerization of mag-N22C enhances binding to vesicles composed of 50% negatively charged lipids by around 2.5-fold.

The use of FPE-labeled vesicles allows binding to be measured under conditions that are very similar to those of the dye release experiments (except that 50 mM *internal* CF is replaced with osmotically equivalent 107 mM NaCl). The fluorescein moiety attached to the phosphatidylethanolamine headgroup has fluorescence properties that are sensitive to local charge and pH. Since the fluorescein group is located near the interfacial region of the bilayer, its fluorescence is highly sensitive to the binding of charged species at the membrane surface as described in detail by O'Shea and his colleagues (*14*). Figure 6b shows that the perturbation of FPE fluorescence, that occurs due to the decreased negative surface charge density on binding of positively charged peptide (*14*), is a linear function of the peptide concentration over the range at which the dye release experiments were made. Figure 6b also shows that vesicle binding is biphasic at high concentrations. This results from access of peptide to the inner bilayer leaflet at high peptide concentrations, and similar observations have been made from isothermal titration calorimetry of magainin peptides binding to vesicles (*24*).

Antimicrobial Activity of Monomeric and Dimeric Magainin Analogues against S. maltophilia and E. coli, and

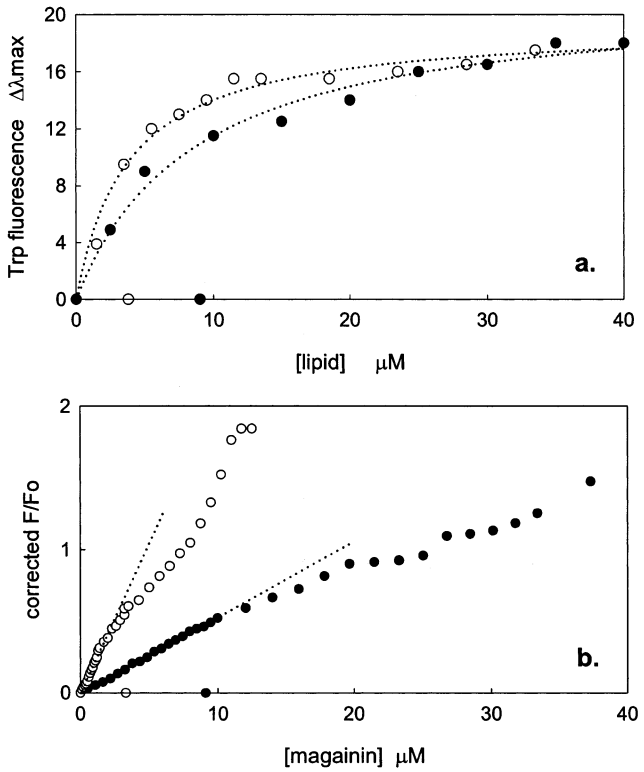

FIGURE 6: Peptide binding to 100 nm LUV (PC/PG; 1:1, M/M) in high salt sample buffer (see text). The top panel (a) illustrates changes in the fluorescence emission maximum of the W12 residue of the peptides upon membrane-binding of the magainin monomer (mag-N22C) (filled circles) and disulfide-linked dimer (open circles) at 2 μM peptide concentration (in *monomer* units). Dotted lines are fits of the binding data to eq 1 with the lipid concentrations for half-maximal binding illustrated on the lipid axis (monomer 9.1 μM lipid; dimer 3.8 μM lipid). The bottom panel (b) illustrates the fraction of the total change in emission intensity, upon peptide binding, of the fluorescein moeity of FPE intercalated in the bilayer of PC/PG LUV in high salt sample buffer (F_o and F are the FPE emission intensities in vesicles in the absence and presence of peptide, respectively). At low concentrations (encompassing the range of peptide concentrations used in the dye-release experiments; see Figures 1 and 2), linear changes in FPE fluorescence are observed with increasing monomer (mag-N22C; filled circles) and disulfide-linked dimer (open circles). Two stages of binding are observed (see text); the peptide concentration corresponding to the half-maximal change in the first binding transition is highlighted for each peptide on the *x*-axis (9 μM monomer; 3.1 μM dimer).

Hemolytic Activity. Comparison of the data in Figures 5 and 7 demonstrates that the high permeabilising activity of (mag-N22C)$_2$ at very low concentrations is reflected in the high antimicrobial activity of the dimer against the Gram negative bacteria *S. maltophilia* and *E. coli*, which is also markedly higher at low concentrations (0.1 μM monomer units) compared to the monomer. Like magainin, mag-N22C has negligible hemolytic activity at concentrations up to at least 50 μM peptide (Figure 8). Disulfide-dimerization significantly enhances hemolytic activity (Figure 8), although this remains negligible at concentrations (1 μM) which produce a 5−6 log reduction in viability of the Gram negative bacteria tested (Figure 7).

DISCUSSION

Disulfide-dimerization of mag-N22C significantly enhances the ability of the peptide to permeabilize vesicles,

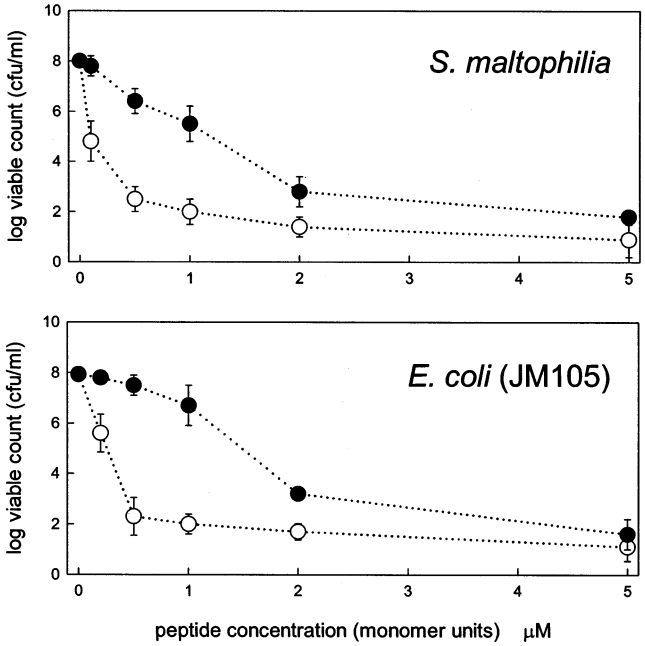

FIGURE 7: Effects of mag-N22C (filled circles) and (mag-N22C)$_2$ (open circles) on the viability of the Gram negative bacterium *S. maltophilia* and *E. coli* in culture. Bacterial cultures were incubated in nutrient broth containing the peptides at the concentrations indicated and counts were obtained after plating. Points are averages with standard deviations, from three experiments.

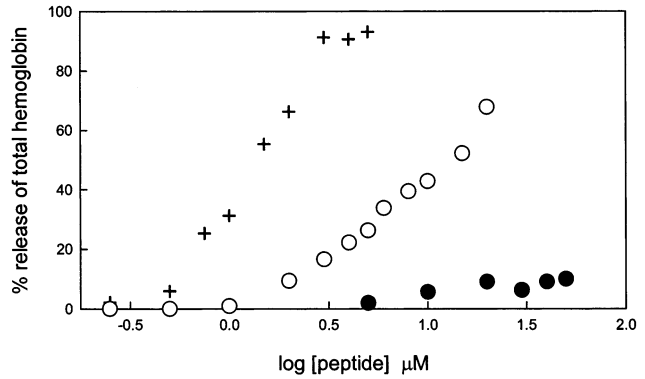

FIGURE 8: Hemolytic activity against human red blood cells for mag-N22C (filled circles), (mag-N22C)$_2$ (open circles), and melittin (crosses). Points are averages of two measurements. The variation between replicates was small and is contained within the size of the symbol in each case.

particularly at very low concentrations. Although a direct relationship between vesicles permeabilization and antimicrobial activity is not established, it is recognized that antimicrobial peptides act at the cell membrane, either killing the cell directly or translocating into the cytoplasm to act on intracellular elements (e.g., *1*, *2*, *25*, *26*). Structure−activity studies of antimicrobial peptides are generally made in relation to their membrane-active properties. The enhanced antimicrobial activity of (mag-N22C)$_2$ against the Gram-negative bacteria *S. maltophilia* and *E. coli* is consistent with the enhanced membrane activity observed in vesicles composed partly of negatively charged lipids.

The relative simplicity of the vesicle system allows the mechanism of vesicle permeabilization to be characterized in more detail. The experiments described here demonstrate that enhanced permeabilization *of vesicles* results from two properties of the dimeric peptide. First, the binding affinity

for negatively charged membranes is enhanced, probably due to the greater net positive charge (+8) of the dimer compared to that of the monomer (net charge of +4). Second, the (mag-N22C)$_2$ dimeric peptide has a lower concentration dependence for permeabilization compared with the monomer. A combination of these effects ensures that at very low concentrations a significant proportion of the total dimeric peptide is bound to the membrane, and that permeabilization is efficient even with rather low amounts of membrane bound peptide dimer.

The sigmoidal dependence of permeabilization on peptide monomer concentration (Figure 5) is consistent with previous observations of cooperativity in pore formation with magainin and its monomeric analogues (*20*, *21*). These authors proposed a toroidal pore comprising magainin helical monomers in a TM orientation with interspersed lipid headgroups (providing a pathway for lipid redistribution among the bilayer leaflets) to yield an aqueous hole of a size sufficient to allow permeation of molecules such as CF (see Figure 5 of each of refs *20* and *21*). While cooperativity is expected to result directly from the requirement for association of multiple monomers to form either a rate-limiting preinsertion complex (*10*), or the pore itself, a sigmoidal dependence of pore formation on peptide concentration might arise from cooperativity in binding of peptide to the membrane (*22*). The data in Figure 6 demonstrate, however, that binding is noncooperative, since each peptide displays hyperbolic binding as determined by vesicle-induced effects on the Trp-16 side chain fluorescence. Similarly, peptide charge-induced perturbation of FPE fluorescence (Figure 6b) is a linear function of the peptide concentration over the concentration range at which each peptide is active in releasing trapped CF. Circular dichroism spectra show that each peptide is unstructured in buffer at concentrations well above those required for permeabilizing vesicles, demonstrating the absence of preassociation before membrane binding. These spectroscopic data, in combination, demonstrate that any cooperativity in formation of the lesion underlying CF release is a result of interactions within the pool of membrane-bound peptide.

Circular dichroism of the membrane-bound peptide confirms that mag-N22C and (mag-N22C)$_2$ (like native magainin) have similar helical contents upon membrane binding. Since previous spectroscopic studies have shown that magainin binds to phospholipid bilayers in the plane of the membrane (parallel to the membrane surface) (*8*) at concentrations below around 1 peptide per 100 lipids, it is likely that the membrane bound helical forms of mag-N22C and (mag-N22C)$_2$ are similarly oriented parallel to the membrane surface. Inspection of a parallel helical dimer oriented with the hydrophobic face containing residues I2, A9, and I20 (see Figure 1) facing the membrane interior, indicates that a disulfide bond between C22 residues on adjacent helices cannot be formed because the residues are too far apart. It is likely that the C-terminal residues are not part of the stable helix in (mag-N22C)$_2$, and that the individual helices in the membrane bound dimer are linked within a flexible C-terminal polypeptide sequence. The C-terminal sequence in the membrane-bound monomeric peptide is also unlikely to be helical beyond residue I20 since residues M21 and S23 do not conform to the helical amphipathic structure of the preceding sequence (Figure 1). This is consistent with the overall helical content (65−70%) of the membrane bound peptides which indicates that around 6 of the 23 residues are not part of the helical structure, and with the observation that dimerization of mag-N22C by disulfide-formation does not affect the CD spectrum of its membrane-associated state.

We have not yet established whether the two helices within membrane-bound mag(N22C)$_2$ are self-associated at equilibrium. The association state of interfacially bound magainins has recently been investigated by Matsuzaki (*27*) who provided evidence for an antiparallel coiled coil dimer for magainin (in neutral PC bilayers), which supports previous evidence for self-association from circular dichroism (ratios of ellipticity at 222 and 208 nm) and observations of positive cooperativity in binding to egg PG vesicles (19). Schümann et al. (*28*), however, found no evidence for self-association of donor and acceptor-labeled magainin-2 amide in vesicles composed of PC/PG (3:1), conditions that are similar to the mixed PC/PG vesicles used in the present study. Since self-association (of the mag-N22C monomer) is expected to yield cooperativity in binding (e.g., refs *19* and *29*), a lack of cooperativity (Figure 6) may be taken to indicate an absence of self-association *at equilibrium* under the conditions of membrane binding and vesicle permeabilization in our experiments. Wenk and Seelig (*24*) also found a lack of cooperativity in binding of magainin-2-amide to PC/PG (3:1) vesicles. Self-association at equilibrium may therefore have a subtle dependence on the magainin analogue studied and the lipid composition. On the other hand, *transient* association of monomers is required to create the toroidal pores of the type previously characterized for magainin (*20*, *21*). The high pore-forming activity of (mag-N22C)$_2$ at very low peptide/lipid ratios, high concentration-dependence in pore-formation of the monomeric peptide, and a reduced concentration-dependence in the dimer, all support a discrete pore mechanism *in vesicles*, in which the self-association properties of the membrane-bound peptides are key determinants in establishing the pore.

A peptide from the skin of an African tree frog has recently been characterized that consists of two potentially amphipathic, helix-forming, positively charged peptides, linked near the C-termini by a disulfide bond (*12*). In line with the observations described here, this peptide is likely to have greater antimicrobial activity compared to the constituent peptide monomers, due to enhanced membrane binding to negatively charged membranes and a lower concentration dependence for membrane permeabilization. It might be predicted that secretion of low concentrations of (hetero-) dimeric peptide may act as a sentinel against the onset of bacterial infection, whereas more serious infections may be better dealt with by the secretion of larger amounts of monomeric peptide. Since monomeric pore forming peptides have a high concentration-dependence for pore formation, pore formation rates can rapidly overtake those of dimers at high peptide concentrations (see Figure 5) to fulfill this role. It remains to be seen whether regulation of peptide secretion may occur in this manner in frog skin. However, the rational design of other homo- or heterodimeric amphipathic helix forming peptides may be a useful approach to generation of novel antimicrobials with useful properties (*30*).

ACKNOWLEDGMENT

We are grateful to Kevin Skinner for preliminary measurements of pore formation with the magainin dimer, Dr. Graham Bloomberg for the excellent synthesis of the magainin monomer, Professor Paul O'Shea for a generous gift of FPE and advice on its incorporation into membranes, and to the Biochemistry Department of Bristol University for financial support of this project.

REFERENCES

1. Hancock, R. E. W., and Lehrer, R. (1998) *Trends Biotechnol. 16*, 82−88.
2. Bevins, C. L., and Zasloff, M. (1990) *Annu. Rev. Biochem. 59*, 395−414.
3. McCafferty, D. G., Cudic, P., Yu, M. K., Behenna, D. C., and Kruger, R. (1999) *Curr. Opin. Chem. Biol. 3*, 672−680.
4. Williams, R. W., Starman, R., Taylor, K. P. M., Gable, K., Beeler, T., and Zasloff, M. (1990) *Biochemistry 29*, 4490−4496.
5. Vaz Gomes, A., de Waal, A., Berden, J., and Westerhoff, H. V. (1993) *Biochemistry 32*, 5365−5372.
6. Matsuzaki, K., Mitani, Y., Akada, K., Murase, O., Yoneyama, S., Zasloff, M., and Miyajima, K. (1998) *Biochemistry 37*, 15144−15153.
7. Hara, T., Mitani, Y., Tanaka, K., Uematsu, N., Takakura, A., Tachi, T., Komada, H., Kondo, M., Mori, H., Otaka, A., Nobutaka, F., and Matsuzaki, K. (2001) *Biochemistry 40*, 12395−12399.
8. Bechinger, B., Zasloff, M., and Opella, S. J. (1993) *Protein Sci. 2*, 2077−2084.
9. Bechinger B., Zasloff M., and Opella S. J. (1998) *Biophys. J. 74*, 981−987.
10. Takei, J., Remenyi, A., and Dempsey, C. E. (1999) *FEBS Lett. 442*, 11−14.
11. Hristova, K., Dempsey, C. E., and White, S. H. (2001) *Biophys. J. 80*, 801−811.
12. Batista, C. V. F., Scaloni, A., Rigden, D. J., Silva, L. R., Rodrigues Romero, A., Dukor, D., Sebben, A., Talamo, F., and Bloch, C. (2001) *FEBS Lett. 494*, 85−89.
13. Denton, M., and Kerr, K. G. (1998) *Clin. Microbiol. Rev. 11*, 57−80.
14. Wall J., Golding C. A., VanVeen, M., and O'Shea, P. (1995) *Mol. Membr. Biol. 12*, 183−192.
15. White, S. H., Wimley, W. C., Ladokhin, A. S., and Hristova, K. (1998) *Methods Enzymol. 295*, 62−87.
16. Schwarz, G., and Arbuzova, A. (1995) *Biochim. Biophys. Acta 1239*, 51−57.
17. Rex, S., and Schwarz, G. (1998) *Biochemistry 37*, 2336−2345.
18. Takei, J., Remenyi, A., Clarke, A. R., and Dempsey, C. E. (1998) *Biochemistry 37*, 5699−5708.
19. Matsuzaki, K., Murase, O., Tokuda, H., Fumakoshi, S., Fujii, N., and Miyajima, K. (1994) *Biochemistry 33*, 3342−3349.
20. Matsuzaki, K., Murase, O., Fujii, N., and Miyajima, K. (1996) *Biochemistry 35*, 11361−11368.
21. Ludtke, S. J., He, K., Heller, W. T., Harroun, T. A., Yang, L., and Huang H. W. (1996) *Biochemistry 35*, 13723−13728.
22. Schwarz, G. (1996) *Biophys. Chem. 58*, 67−73.
23. Ladokhin, A. S., Jayasinghe, S., and White, S. H. (2000) *Anal. Biochem. 285*, 235−245.
24. Wenk, M. R., and Seelig, J. (1998) *Biochemistry 37*, 3909−3916.
25. Hancock, R. E. W., Falla, T., and Brown, M. (1995) *Adv. Microb. Physiol. 37*, 135−175.
26. Zasloff, M. (2002) *Nature 415*, 389−395.
27. Wakamatsu, K., Takeda, A., Tachi, T., and Matsuzaki, K. (2002) *Biopolymers 64*, 314−327.
28. Schümann, M., Dathe, M., Wieprecht, T., Beyermann, M., and Bienert, M. (1997) *Biochemistry 36*, 4345−4351.
29. Schwarz, G. (2000) *Biophys. Chem. 86*, 119−129.
30. Tencza, S. B., Creighton, D. J., Yuan, T., Vogel, H. J., Montelaro, R. C., and Mietzner, T. A. (1999) *J. Antimicrob. Chemother. 44*, 33−41.

BI026328H